Osteosarcoma cells relate functionally with stromal cells favoring a lung niche permissive for the establishment of metastatic tumor cells

Matías J.P. Valenzuela Alvarez
Instituto de Medicina Traslacional e Ingeniería Biomédica (IMTIB), CONICET - Hospital Italiano Buenos Aires (HIBA) - Instituto Universitario del Hospital Italiano (IUHI), CABA (C1199ACL)

Luciana M. Gutierrez
Instituto de Medicina Traslacional e Ingeniería Biomédica (IMTIB), CONICET - Hospital Italiano Buenos Aires (HIBA) - Instituto Universitario del Hospital Italiano (IUHI), CABA (C1199ACL)

Juan Bayo
IIMT – CONICET, Universidad Austral

María José Cantero
IIMT – CONICET, Universidad Austral

Mariana Garcia
IIMT – CONICET, Universidad Austral

Marcela F Bolontrade (marcela.bolontrade@hospitalitaliano.org.ar)
Instituto de Medicina Traslacional e Ingeniería Biomédica (IMTIB), CONICET - Hospital Italiano Buenos Aires (HIBA) - Instituto Universitario del Hospital Italiano (IUHI), CABA (C1199ACL)

Research Article

Keywords: Osteosarcoma, metastasis, migration, mesenchymal stem cells, mesenchymal stromal cell, invasion, MMP2

Posted Date: October 24th, 2023

DOI: https://doi.org/10.21203/rs.3.rs-3471838/v1

Additional Declarations: No competing interests reported.

Abstract

Osteosarcoma (OS) is the most common bone tumor and 20% of the patients are diagnosed with metastatic OS at first diagnosis. Undetectable metastases at the time of diagnosis are also a major complication. MSCs display abilities that enable tumor growth. We demonstrated that in vitro, MSCs migrated more towards the secretome of non-metastatic OS cells. When challenged to a secretome from lungs pre-loaded with OS cells, MSCs migrated more towards lungs colonized with metastatic OS cells. Furthermore, MSCs had a preferential migratory and homing behavior in vivo towards lungs´ colonized by metastatic OS cells. In addition, metastatic OS cells showed a higher migratory response towards the MSCs secretome. This feature partnered with increased CTSD expression and release of active MMP2 by metastatic OS cells. We assessed two complementary tumor capabilities relevant to metastatic spread, highlighting the importance of inherent cell features, but also underlining the importance of signaling integration across the niche, suggesting that an interplay of migratory responses between already established OS cells in the lungs, prometastatic OS cells in the primary tumor, and circulating MSCs. Pulmonary metastases remain as a major determinant of OS mortality, and identification of mechanisms and differentially expressed genes would help identify markers and targets for therapeutic approaches of metastatic spread.

Introduction

A key feature of malignant tumor progression is the appearance of detectable metastasis, which represents a major clinical complication in the cancer treatment scenario. The two key biological aspects that support and enable the spread of tumor cells from the primary location are migration and invasion. Although they are connected in an intricate and complex way that sometimes leads to the same biological goal, these processes have distinct features. Tissue invasion and metastasis have been recognized as cancer hallmarks by Hanahan and Weinberg, and in 2010 Labeznik highlighted their importance as the only two features able to differentiate a benign from a malignant tumor [1–3]. Invasion is a biological process in which several actors are involved, mainly proteins with the ability to modify the extracellular matrix (ECM), such as metalloproteinases (MMPs) or cathepsins (CTSs) [4, 5]. Tumor cells spread to distant sites require cell migration, which is governed by the influence of different chemotactic axes such as CXCR4-CXCL12 or CCR2-CCL2 [6–8]. Metastasis as the advanced stage of cancer spread, is the leading cause of mortality and morbidity, accounting for 90% of cancer-related deaths [9]. In this scenario, tumors with rapid progression and metastatic ability become relevant.

Osteosarcoma (OS) is the most common bone tumor with a predominant pulmonary metastasis pattern. OS metastases exist early in tumor progression. Even when twenty percent of OS patients are first diagnosed with metastatic OS, it is estimated that 80% of patients diagnosed with OS would have undiagnosed micrometastasis at that time [10–13]. Since the 1970s, patients with metastatic disease have not presented significant changes in the 5-year survival rate of 15–30%. The appearance of micrometastases represents a major complication since they are not detectable by conventional methods [14].

Given the tissue context where OS arises, mesenchymal stem/stromal cells (MSCs) represent a population of interest in different aspects. MSCs are multipotent stem cells that possess characteristics that allow them to support tumor growth [15]. In addition, we have previously demonstrated that the stromal component in the OS microenvironment modifies the tumor cells and MSCs stemness state, according to the tumor context [16, 17]. Given their pleiotropic role, MSCs have been involved in several cancer models as participants in almost all of the cancer hallmarks, highlighting their role as components of the tumor microenvironment [18–20]. The pathological bone scenario established during OS onset and progression involves a complex signaling and molecular release between tumor cells and the bone-altered niche. During pulmonary metastatic spread, OS cells within the primary tumor site could acquire metastatic traits such as migratory and invasion capacity. Likewise, those complex modifications in the stroma could exert a selection pressure over previously residing OS subpopulations with differential abilities, thus favoring cells with metastatic traits to leave the nest towards future metastatic sites.

In this schema, we primarily focused on the interrelated modulation between MSCs and OS cells and the resulting migratory pattern associated with primary and metastatic settings. We demonstrated that MSCs have a migratory pattern in vitro, that favors a response towards the secretome of non-metastatic OS cells. When challenged with secretomes from lungs pre-loaded with OS cells, MSCs displayed a migratory response favoring lungs colonized with metastatic OS cells. We have previously demonstrated that MSCs incorporate into different tumor stromas [21, 22]. To put this migratory response towards a complex secretome into perspective, we showed in this model that MSCs migrate to and home to OS lung metastatic areas. This proof of concept for the importance of MSCs as metastatic supportive stromal components of OS, suggests that categorizing a single cell or group of cells as metastatic or non-metastatic by eliciting a given biological response within their immediate surrounding conditions, is ultimately modulated by the whole niche. In addition, metastatic OS cells showed a higher migratory response towards MSCs´ secretome. This feature partnered with increased production of pro-MMP2 and cathepsin D, and by the release of active MMP2 by metastatic OS cells. Cancer progression involves multistep functional events, which may ultimately lead to the acquisition of a metastatic phenotype. We assessed two complementary tumor capacities relevant for metastatic spread, highlighting the importance of inherent cell features that allow a cell to colonize a distant organ, but also underlined the importance of niche-wide signaling integration, suggesting that an interplay of migratory responses between OS cells already established in the lungs, prometastatic OS cells in the primary tumor, and circulating MSCs, will ultimately lead to the successful growth of the secondary tumor. Hence, the metastatic secretome was capable of inducing a differential migratory response in MSCs, but also the MSCs secretome induces a differential migration in OS cells with distinct metastatic abilities. Pulmonary disease remains as a major OS mortality determinant, and identification of mechanisms and differentially expressed genes associated with metastasis would help in discovering promising markers and targets for therapeutic approaches for OS metastatic spread.

Materials and Methods

Cell lines

Human OS cell lines were supplied by Dr. Kleinerman, MD Anderson Cancer Center (MDACC). Cells were grown in Dulbecco's Modified Eagle Medium: Nutrient Mixture F12 (DMEM/F12) supplemented with 2mM L-glutamine, 100 U/mL penicillin, 100 mg/mL streptomycin (Invitrogen), 10% fetal bovine serum (FBS; Natocor), at 37°C, 5% CO_2. SAOS2 is a cell line established from a primary tumor in the seventies, while LM7 cells have been selected from parental SAOS2 cells by their metastatic ability through lung cyclic circulation, ability associated to avoidance of apoptosis and apoptosis-resistance mechanisms [23]. Human microvascular endothelial cells HMEC-1 (Dr. Candal, Centers for Disease Control, Atlanta) were grown in DMEM/F12, 10% FBS (Natocor), 2 mM L-glutamine, 100 U/mL penicillin, and 100 mg/mL streptomycin. Human MSCs were isolated from bone marrow (BM) aspirates collected from posterior iliac crest from healthy donors for BM transplantation after informed consent (Institutional Review Committee approval #1497). Mononuclear cells collected from Ficoll–Hypaque gradient (Sigma-Aldrich) were plated in low-glucose DMEM (DMEM low, Invitrogen), 20% FBS (Internegocios S.A.). MSCs were used from passages 2 to 4 [21]. Verification of mycoplasma species was carried out (MycoAlert Mycoplasma Detection Kit, Lonza Inc.).

Cell Conditioned Medium

The cells´ secretome compartment is represented by their conditioned medium (CM). Cells were seeded on 100 mm culture dishes until 80% confluence, washed with phosphate basic solution (PBS) and cultured during twenty-four hours with basal medium (DMEM or DMEM/F12). After this the CM was collected, centrifuged for 5 minutes (1200 rpm), aliquoted and stored at -80ºC until use. Conditioned medium was also produced from mice lungs. Briefly, nude mice (nu/nu, NIH) which were previously injected with 1×10^6 LM7 or SAOS2 cells/200 µl PBS intravenously (i.v, lateral tail vein) resulting in microscopic lung metastases development or not. For the control group, 200 µl of physiological solution was injected intravenously (i.v, lateral tail vein). Lungs were dissected and minced into pieces smaller than 1 mm^3 and transferred to a 24-well tissue culture plate (6 fragments/well) with 500 µL of complete DMEM without FBS. Twenty-four hours later CM was harvested and stored at -80ºC until use.

In vitro migration assays

In vitro cell migration was assayed for 4 h, 37ºC (modified Boyden chamber, Neuroprobe). Cells were cultured until 70% – 90% confluence and seeded on the chamber´s upper wells ($1.2x10^4$ cells/50 µL DMEM). Cells that responded to chemotactic stimuli (lower well, 28 µL) migrated through 8-um-pore polycarbonate filters (Neuroprobe Inc.). Basal medium was used as negative control. After the assay, cells were scraped-off the upper side of the filter. Cells attached to the lower side were fixed (4% paraformaldehyde, PFA) and stained (4,6-Diamidino-2-phenylindole dihydrochloride, DAPI, Sigma-Aldrich). Images were captured from 2 visual fields covering the whole well (fluorescent-field microscopy, Olympus) and cells were counted (mean number of cells/field ± SD), (ImageJ software, National Institutes of Health, NIH, Bethesda, MD).

Gelatin Zymography assay

To evaluate gelatinolytic activity, $5x10^4$ cells were seeded in 24-well plates. Cells at 80% confluence were washed (PBS) and cultured in serum-free DMEM, 1 g/L glucose (6 h) before collecting supernatants. The positive control was CM from HT1080 cells. MMP2 and MMP9 activity was determined by zymography. Briefly, cell cultures supernatants (40 µL) were run on a 10% SDS PAGE gel containing 0.1% gelatin (Sigma-Aldrich). Gel was stained (Coomassie Brilliant Blue R-250, 30 min, room temperature). Gelatinase activity was visualized by negative staining; gel images were obtained (digital camera, Canon EOS 5D), and subjected to densitometry analysis (Scion Image software, Scion Corporation, MD). Relative pro and active-MMP2 values were obtained by normalizing values to positive control samples (CM of HT1080).

Reverse Transcription-polymerase Chain Reaction (RTPCR) and Real Time polymerase Chain Reaction (qPCR)

Total RNA from OS cells (Trizol Reagent, Molecular Research Center, USA) was reverse transcribed (2 µg) with 200 U of *Easy Script* Reverse Transcriptase (Transgenbiotech) using Oligo (dT) primers (500 ng). cDNAs were subjected to qPCR (CFX96 Touch TM Real-Time PCR Detection System, Bio-Rad). Cathepsin A (CTSA), Cathepsin D (CTSD), Matrix Metalloproteinase-2 (MMP2), mRNA levels were quantified (SYBR Green, Roche) using the following primers: CTSA forward 5´ACGCCAGCCAACTGTGATCCT3´, reverse 5´ATATGCGGCATCCACGCCTGAA3´; CTSD forward 5´ ACAAGATGTGGGCCTTGCAAGA3´, reverse 5´AAAACGCAGTGCTCCCAGGATA3´; MMP2 forward 5´CCAGCCAGAAGCGGAAACTT3´, reverse 5´TGACCTTTCCAGCAGACACC3´. PCR amplification was carried out using a 95ºC for 10 min cycle and 40 cycles under the parameters: 95ºC for 20 sec, 60ºC for 1 min, 72ºC for 40 sec and a 95ºC for 20 sec cycle. At the end the temperature was increased from 60ºC to 95ºC (2ºC/min rate), and fluorescence was measured every 15 sec to construct the melting curve. Values were normalized to levels of glyceraldehyde-3-phosphate dehydrogenase (GAPDH) mRNA levels, forward 5' GGGGCTGCCCAGAACATCAT 3', reverse 5' GCCTGCTTCACCACCTTCTTG 3'. Data were processed by the DDCt method. A non-template control (NTC) was run in every assay; all determinations were performed as triplicates in three separated experiments.

In vivo assays

Animal experiments were approved by the Institutional Animal Care and Use Committee (IACUC IMTIB 0001/19). Four to six-week-old athymic male nude mice were i.v. injected with 1×10^6 LM7 cells /200 µl PBS (lateral tail vein) resulting in microscopic lung metastases. MSCs were labeled with DiR (infrared lipophilic tracker, Invitrogen) following manufacturer instructions. DiR^+ MSCs ($0.5x10^6$ cells/200 µL PBS) were i.v. administered 10 weeks after tumor cell injection. MSCs biodistribution and homing analysis was evaluated through real-time analysis. DiR *in vivo* tracking detection was followed by Fluorescence Imaging (FI) IVIS Lumina Bioluminometer (Xenogen). For FI analysis, captured images were measured as average photons per sec per square centimeter per steradian ($p/sec/cm^2/sr$).

Bioinformatics analysis

The GSE14359 dataset was downloaded from the Gene Expression Omnibus (GEO) database (https://www.ncbi.nlm.nih.gov/gds/). The GSE14359 consists of mRNA from 5 frozen conventional osteosarcoma and 4 osteosarcoma lung metastases tumor samples and mRNA from fresh primary osteoblast cells, and each sample was analyzed by duplicate. The program R2 (http://r2.amc.nl) was used to analyze and visualized specific genes from the dataset Mixed Osteosarcoma – Guenther – 20 – MAS5.0 – u133a (also GSE14359 from GEO database) [24]. The gene expression was analyzed based on primary versus metastatic status. Kaplan-Meier survival curves for metastasis-free survival rates were also created with the R2 program based on the dataset Mixed Osteosarcoma (Mesenchymal) – Kuijjer – 127 – vst – ilmnhwg6v2 (also GSE42352 from GEO database) [25].

Statistical Analysis

95% confidence intervals (CI) were determined by calculating arithmetic mean values and variance (standard deviation, SD) of three independent experiments. Unpaired 2-sided Student's t test (two groups comparisons) and analysis of variance (ANOVA) followed by post-tests Kruskal-Wallis and Dunn's post-tests (more than two experimental groups comparisons) (GraphPad Prism Software, San Diego, CA) were used for statistical analyses, considering p value < 0.05 as statistically significant.

Results

Chemotactic crosstalk between parenchymal and stromal cell in OS

To assess the effects exerted by SAOS2 and LM7 cells on functions relevant to the cell stromal compartment, the response of MSCs towards CM of OS cell lines was evaluated through *in vitro* migration assays. Results showed that MSCs responded to chemotactic signals present in both SAOS2 and LM7 CM (Fig. 1A). However, SAOS2 cells' secretome induced a 1.5-fold significantly higher chemotactic effect on MSCs as compared to the migration exerted by LM7 cells' secretome. This higher chemoresponse towards the non-metastatic cell line was shared by other stromal cells. Human microvascular endothelial cells (HMEC-1) displayed the same tendency, with a 1.3-fold increased chemotactic response towards SAOS2 secretome (Fig. 1B). On the other hand, when OS cells were challenged with the chemotactic stimuli from MSCs, LM7 cells showed a 2-fold increase in their migratory response towards MSC´s secretome compared to SAOS2 cells (Fig. 1C).

In vivo context complexity signaling determines migration of stromal populations

In order to assess the potential relevance of the microenvironment, we evaluated the chemotactic effect of CM from lungs belonging to animals previously injected with SAOS2 (CML + S) or LM7 (CML + L) cells, through *in vitro* migration assays (Fig. 2A). Interestingly and in contrast to the results obtained from CM under cell-only in vitro conditions, MSCs exhibited a significantly higher chemotactic response trend

towards CM from lungs with LM7 cells compared to CM from lungs with SAOS2 cells (1.69-fold vs 1.06, CML + L and CML + S respectively) (Fig. 2B and C). Since this difference could be partly attributed to the added complexity of the *in vivo* lung microenvironment created by the presence of metastatic cells, we analyzed the dataset GSE14359 which is a transcriptomic database of human OS primary and metastatic tissue and normal osteoblasts. Focusing on the changes involved in an inflammatory context, we selected 4 candidates CXCR4 (C-X-C chemokine receptor type 4), S100A14, IL-1α (interleukin 1 alpha), and PECAM1 (platelet-endothelial cell adhesion molecule 1). These genes are implicated in migration, pulmonary inflammation, overall inflammation, and adhesion, respectively. S100A14 and PECAM1 had significantly higher expression in metastatic samples, while CXCR4 and IL-1α displayed a similar trend but with no statistical significance (Fig. 2D and E).

Incorporation of systemically delivered MSCs into secondary tumor growth sites

In view of the relevance of the microenvironment, we evaluated the environment contribution, in addition to the ability of the tumor cell itself, in the recruitment of MSC to a metastatic lung site. We performed an in vivo assay as a proof of concept of the microenvironment as a chemotactic response modulator (Fig. 3A). In this context, we evaluated the in vivo migration of MSCs in lungs with and without metastatic cells. LM7 cells were intravenously (i.v.) injected into immunosuppressed mice. Pre-labeled MSCs (DiR^+, 0.5-1x10^6 cells) were i.v. administered 10 weeks after tumor cells injection. MSCs biodistribution was evaluated through whole body DiR signal detection (Fig. 3B). Labeled MSCs levels one-week post-inoculation were higher in the lungs of tumor-bearing mice than in mice with non-tumor burden (Fig. 3C and D). This was indicative of a high homing ability of MSCs in the metastatic tumor microenvironment. Suggesting that the presence of LM7 cells within the lungs would favor a favorable lung niche involving MSCs recruitment. In addition, infrared-tagged (DiR^+) MSCs displayed heterogeneous distribution in the LM7 lungs, suggesting a chemo-attractive and homing behavior towards localized areas in the tumor-cell bearing lungs (Fig. 3C).

Expression and activity of matrix metalloproteinases and Cathepsins in OS cells

Tissue remodeling, which involves the recruitment of cells from the local tissue environment and from distant tissues, aids in the development of a suitable niche for the growth of primary tumors and metastases. An important trait of metastatic cells is the ability to modify and alter the extracellular matrix (ECM). Aiming to evaluate the capacity of OS cells to modify the ECM, we analyzed their ability to secrete active MMPs, MMP2 and MMP9 activities were assayed by SAOS2 and LM7 secretome zymography. We demonstrated the lack of MMP2 release in non-metastatic cells, while metastatic LM7 cells had the ability to release pro and active MMP2 (Fig. 4A, B and C). No MMP9 activity was detected in OS cells. We addressed MMP2 expression in OS cells, with LM7 cells expressing MMP2 while parental SAOS2 cells had no significant levels of expression at the mRNA level (Fig. 4D). Interestingly, generation of Kaplan–

Meier metastasis-free survival curve using the R2: Genomics Analysis and Visualization Platform (Acad Med Center, Amsterdam) indicated that high MMP2 expression was correlated with diminished metastasis free survival rate pointing at MMP2 role in the establishment of a metastatic niche (Supp. Figure 1). Further, Cathepsin D was found differentially expressed in LM7 cells by qPCR (3,5-fold increase), while Cathepsin A did not show differences at mRNA expression levels. These results suggest that LM7 presents a higher expression of molecules functionally related to ECM remodeling and invasion (Fig. 4D).

Discussion

Despite therapeutic combinations, the five-year survival rate for OS remains at 60–70%, and patients with pulmonary metastases at diagnosis have a survival rate of 15–30% for the last thirty years [26]. The tumor niche is established through the interplay between tumor cells, cancer stem cells, stromal cells and the extracellular matrix, generating genetic and phenotypic cell divergence [27]. In particular, MSCs contribute to the stromal compartment adding to the structural and functional microenvironment [28].

Metastasis represents a complex biological process that involves several biological features such as invasion, chemotaxis and migration, just to mention a few key metastatic abilities. In order to elucidate if the metastatic ability in LM7 cells was functionally related to other cells in the tumor niche, we assessed migratory and invasive capacity on tumor and stromal cells. Metastatic potential involves the remodeling of the extracellular matrix (ECM) as a key step. During this process, two families of proteins are relevant, metalloproteinases (MMPs) and cathepsins (CTSs). We demonstrated LM7 metastatic potential by gelatin zymography assessing MMP2 and MMP9 activity. MMP2 and MMP9 have been previously reported to be directly associated with high grade OS and metastatic potential [29]. We demonstrated that the CM from LM7 had MMP2-gelatinase activity, while SAOS2 CM did not show this activity. Neither of the two OS cell lines showed MMP9 activity or PRO-MMP9 presence. Interestingly, at the mRNA level, SAOS2 displayed significantly higher levels of PRO-MMP2 expression compared to LM7, suggesting a possible regulatory mechanism. In this context, the metastasis-free survival curve of MMP2 showed that higher expression is associated with a lower probability of metastasis free survival (Supp. Figure 1). We analyzed the expression of CTSA and CTSD, which are two proteins involved in ECM remodeling. Even though we detected no differences in CTSA expression between the cell lines, CTSD was significantly upregulated in LM7 cells, showing a 3,5-fold increase in expression compared to SAOS2 cells. CTSD has been implicated in tumor invasion and metastasis in different tumor models and has also been proposed as a possible biomarker of OS [30, 31]. CTSD, which is increased in metastatic cells, has also been reported to have a role in protecting against apoptosis [14].

Migratory responses are important during tumor progression. Tumor cells rely on an enhanced migratory response for metastasis to occur, an ability required to intra- and extravasation and tissue invasion, sustaining tumor growth in different anatomic locations [32]. Interestingly, secretomes from OS cells induced a differential migratory effect on MSCs. While both types of tumor cells produce a secretome capable of stimulating MSCs migration, SAOS2 cells showed significantly enhanced avidity in recruiting

MSCs. Other stromal components such as microvascular endothelial cells, show a similar migration pattern towards OS cells, highlighting a possible differential role of MSCs in niche formation [16]. On the other hand, LM7 cells had a higher migratory response towards MSCs. This would relate to LM7 cells ability to metastasize and, in particular, suggests that metastatic OS cells home into lungs previously colonized by MSCs. In this scenario, the development of lung metastases could be associated with a permissive niche provided by MSCs previously incorporated into the lungs, lung-residing MSCs, or by exosomes released by tumor-educated MSCs [17, 18]. In this microenvironmental context, OS cells with advantageous abilities to leave the primary tumor would respond to a permissive “soil” induced by MSCs in the lungs [33]. As such, enhanced migration and the ability to degrade ECM were both traits upregulated in metastatic OS cells (Fig. 5). Metalloproteinase 2 has been shown to promote stemness [19, 20]. In this context, we had previously shown that metastatic OS cells have an increased capacity to modify the intracellular localization of chemotherapy drugs, and a decreased intrinsic osteoblastic differentiation potential, traits associated with stemness states [21]. Interestingly, a role of MMP2 as a stemness-enabling factor could contribute to the matrix remodeling function of this protein in the metastatic environment. In this scenario, increased MMP2 in LM7 cells may not only allow invasion, but may also have a different role in providing a supportive and favorable environment for the survival of metastatic cells.

In this model, LM7 cells (representative of OS metastasis), derived from Fas^+ SAOS2 cells (representative of primary OS tumor), are able to establish secondary tumor growth in the lungs and display inappreciable levels of Fas (Fas^-). Fas + OS cells are not fit for colonizing the FasL + lung environment and Fas − LM7 cells establish pulmonary metastases, as previously demonstrated. This relates to clinical observations in which the primary OS tumor expresses high levels of Fas, while OS lung metastases have inappreciable Fas expression [23, 34]. Furthermore, the imbalance in bone homeostasis associated with OS onset greatly affects and is affected by MSCs as master regulators of bone physiology [35, 36]. From our results, a picture emerges depicting a heterogeneous OS primary tumor that avidly recruits stromal cells. Some of the tumor cell subpopulations would leave the primary tumor and colonize the lungs in response to a suitable niche and stimuli, ie, lung MSCs, and probably further attracting more MSCs to the lungs (Fig. 5). The identified signaling events mediated by different molecules such as CXCR4, S100A14, IL-1α and PECAM1 (Fig. 2D and E), are in agreement with the bidirectional migration interplay observed between MSCs and OS cells [28]. A pathologic bone remodeling scenario emerges, with the selection of advantageous properties, resulting in both MSCs and OS cells being able to foster the conditions for a secondary tumor site in a coordinated manner. Furthermore, a molecular pattern associated with migration and invasion is present in cells with divergent metastatic potential. These cells would at first reside together at the primary site, but are enabled with differential abilities to leave the primary tumor and colonize the lungs. The identification of novel molecules in OS cells with metastatic features would permit the validation of molecules with usefulness as a biomarker in a disease in which the existence of undetectable lung micrometastases present at diagnosis time remains a critical clinical challenge.

Conclusions

We present a functional and molecular comparison between a parental non-metastatic OS cell line and a derived-metastatic cell line selected for lung colonization behavior, and propose aa model of OS cells - MSCs interaction at primary and secondary tumor growth sites. Our results showed that subtle molecular modifications in the metastatic tumor cells allow metastatic colonization of the lungs. Furthermore, metastatic and non-metastatic OS secretomes differentially modulate the stroma, and OS cells establish a distinct functional interaction with mesenchymal stem cells. Metastatic OS cells would create a niche that would ensure tumor establishment in the lungs.

Abbreviations

BM Bone marrow

CCL2 C-C motif chemokine ligand 2

CCR2 C-C motif chemokine receptor 2

CM Conditioned medium

CTSA Cathepsin A

CTSD Cathepsin D

CTSs Cathepsins

CXCR4 C-X-C motif chemokine receptor 4

CXCL12 C-X-C motif chemokine ligand 12

DAPI 4´, 6-Diamidino-2-phenylindole

DMEM Dulbecco´s modified eagle´s medium

DMEM/F12 Dulbecco´s modified eagle´s medium/ Nutrient mixture F12

ECM Extracellular matrix

FBS Fetal bovine serum

FI Fluorescence intensity

HMEC-1 Human microvascular endothelial cells

MMPs Metalloproteinases

MMP2 Metalloproteinase 2

MMP9 Metalloproteinase 9

MSCs Mesenchymal stem cells

qPCR Real time polymerase chain reaction

PBS Phosphate buffer solution

OS Osteosarcoma

References

1. Hanahan D, Weinberg RA (2000) Tha hallmarks of cancer. 100(1):57–70
2. Lazebnik Y (2010) What are the hallmarks of cancer? Nat Rev Cancer 10(4):232–233
3. Friedl P, Wolf K (2003) Tumour-cell invasion and migration: diversity and escape mechanisms. Nat Rev Cancer 3(5):362–374
4. Vidak E, Javoršek U, Vizovišek M, Turk B (2019) Cysteine Cathepsins and their Extracellular Roles: Shaping the Microenvironment. Cells 8(3):264
5. Murphy G, Nagase H (2011) Localizing matrix metalloproteinase activities in the pericellular environment. FEBS J 278(1):2–15
6. Bogenrieder T, Herlyn M (2003) Axis of evil: molecular mechanisms of cancer metastasis. Oncogene 22(42):6524–6536
7. Tulotta C, Stefanescu C, Chen Q, Torraca V, Meijer H, Snaar-Jagalska B (2019) CXCR4 signaling regulates metastatic onset by controlling neutrophil motility and response to malignant cells. Sci Rep 9(1):2399
8. Lim SY, Yuzhalin AE, Gordon-Weeks AN, Muschel RJ (2016) Targeting the CCL2-CCR2 signaling axis in cancer metastasis. Oncotarget 7(19):28697–28710
9. Seyfried TN, Huysentruyt LC (2013) On the Origin of Cancer Metastasis. Crit Reviews Oncol 18(1–2):43–73
10. Marko TA, Diessner BJ, Spector LG (2016) Prevalence of metastasis at diagnosis of osteosarcoma: an international comparison. Pediatr Blood Cancer 63(6):1006–1011
11. Sheng G, Gao Y, Yang Y, Wu H (2021) Osteosarcoma and Metastasis. Front Oncol 11:780264
12. Strauss SJ, Ng T, Mendoza-Naranjo A, Whelan J, Sorensen PH (2010) Understanding micrometastatic disease and Anoikis resistance in ewing family of tumors and osteosarcoma. Oncologist 15(6):627–635
13. Bruland OS, Høifødt H, Saeter G, Smeland S, Fodstad O (2005) Hematogenous micrometastases in osteosarcoma patients. Clinial Cancer Research 11(13):4666–4673
14. Mao X, Mei R, Yu S, Shou L, Zhang W, Li K et al (2022) Emerging Technologies for the Detection of Cancer Micrometastasis. Technol Cancer Res Treat 21:1–11

15. Studeny M, Marini FC, Dembinski JL, Zompetta C, Cabreira-Hansen M, Nebiyou Bekele B et al (2004) Mesenchymal stem cells: potential precursors for tumor stroma and targeted-delivery vehicles for anticancer agents. J Natl Cancer Inst 96(21):1593–1603
16. Valenzuela Alvarez M, Gutiérrez LM, Auzmendi J, Correa A, Lazarowski A, Bolontrade MF (2020) Acquisition of stem associated-features on metastatic osteosarcoma cells and their functional effects on mesenchymal stem cells. Biochim Biophys Acta Gen Subj. Jan 13. 2020;1864(4)
17. Gutiérrez LM, Valenzuela Alvarez M, Yang Y, Spinelli F, Cantero MJ, Alaniz L, García MG, Kleinerman ES, Correa A, Bolontrade MF (2021) Up-regulation of pro-angiogenic molecules and events do not relate with an angiogenic switch in metastatic osteosarcoma cells but to cell survival features. Apoptosis. May 22. 2021;26(7–8):447–59
18. Weinberg RA, Hanahan D (2011) Hallmarks of Cancer: The Next Generation. Cell. ;144
19. Pietras K, Östman A (2010) Hallmarks of cancer: Interactions with the tumor stroma. Sci Direct 316:1324–1331
20. Hanahan D, Coussens LM (2012) Accessories to the crime: functions of cells recruited to the tumor microenvironment. Cancer Cell 21(3):309–322
21. Bolontrade MF, Sganga L, Piaggio E, Viale DL, Sorrentino MA, Robinson A et al (2012) A specific subpopulation of mesenchymal stromal cell carriers overrides melanoma resistance to an oncolytic adenovirus. Stem Cells Dev 21:2689–2702
22. Bayo J, Fiore E, Aquino JB, Malvicini M, Rizzo M, Peixoto E et al (2014) Increased Migration of Human Mesenchymal Stromal Cells by Autocrine Motility Factor (AMF) Resulted in Enhanced Recruitment towards Hepatocellular Carcinoma. PLoS One [Internet]. ;9(4):e95171. Available from: http://www.ncbi.nlm.nih.gov/pubmed/24736611
23. Jia S, Worth LL, Kleinerman ES (1999) A nude mouse model of human osteosarcoma lung metastases for evaluating new therapeutic strategies. Clin Experimental Metastasis 17:501–506
24. Fritsche-Guenther R, Noske A, Ungethüm U, Kuban RJ, Schlag PM, Tunn PU et al (2010) De novo expression of EphA2 in osteosarcoma modulates activation of the mitogenic signalling pathway. Histopathology 57(6):836–850
25. Kuijjer ML, Rydbeck H, Kresse SH, Buddingh EP, Lid AB, Roelofs H, Bürger H, Myklebost O, Hogendoorn PC, Meza-Zepeda LA, Cleton-Jansen AM (2012) Identification of osteosarcoma driver genes by integrative analysis of copy number and gene expression data. Genes Chromosomes Cancer 51(7):696–706
26. Bielack SS, Kempf-Bielack B, Delling G, Ulrich Exner G, Flege S, Helmke K et al (2002) Prognostic Factors in High-Grade Osteosarcoma of the Extremities or Trunk: An Analysis of 1,702 Patients Treated on Neoadjuvant Cooperative Osteosarcoma Study Group Protocols. J Clin Oncol 20(3):776–790
27. Nowell P (1979) The clonal evolution of tumor cell populations. Science 1976;194(4260):23–8
28. Spaeth E, Dembinski J, Sasser A, Watson K, Klopp A, Hall B et al (2009) Mesenchymal Stem Cell Transition to Tumor-Associated Fibroblasts Contributes to Fibrovascular Network Expansion and

Tumor Progression. PLoS ONE 4(4):11

29. Ali N, Venkateswaran G, Garcia E, Landry T, McColl H, Sergi C et al (2019) Osteosarcoma progression is associated with increased nuclear levels and transcriptional activity of activated β-Catenin. Genes Cancer 10(3–4):63–79
30. Zhang C, Zhang M, Song S (2018) Cathepsin D enhances breast cancer invasion and metastasis through promoting hepsin ubiquitin-proteasome degradation. Cancer Lett 438:105–115
31. Gemoll T, Epping F, Heinrich L, Fritzsche B, Roblick UJ, Szymczak S et al (2015) Increased cathepsin D protein expression is a biomarker for osteosarcomas, pulmonary metastases and other bone malignancies. Oncotarget 6(18):16517–16526
32. Hendrix MJ, Seftor EA, Chu YW, Trevor KT, Seftor RE (1996) Role of intermediate filaments in migration, invasion and metastasis. Cancer Metastasis Rev 15(4):507–525
33. Langley RR, Fidler IJ (2011) The seed and soil hypothesis revisited–the role of tumor-stroma interactions in metastasis to different organs. Int J Cancer 128(11):2527–2535
34. Lafleur NV, Stewart J, Jia SF, Worth LL, Duan X, Kleinerman ES (2004) EAK. Increased Fas Expression Reduces the Metastatic Potential of Human Osteosarcoma Cells. Clinical Cancer Research. Dec 1 2004;10(23):8114–9
35. Siddiqui JA, Partridge NC (2016) Physiological Bone Remodeling: Systemic Regulation and Growth Factor Involvement. Physiol (Bethesda) 31(3):233–245
36. Bussard KM, Spaeth E, Mutkus LA, Stumpf KA, Marini FC (2017) Mesenchymal Stem Cell Transition to Tumor-Associated Stromal Cells Contributes to Cancer Progression. In: Bolontrade MF, Garcia MG (eds) Mesenchymal Stromal Cells as Tumor Stromal Modulators. Elsevier, pp 253–273

Figures

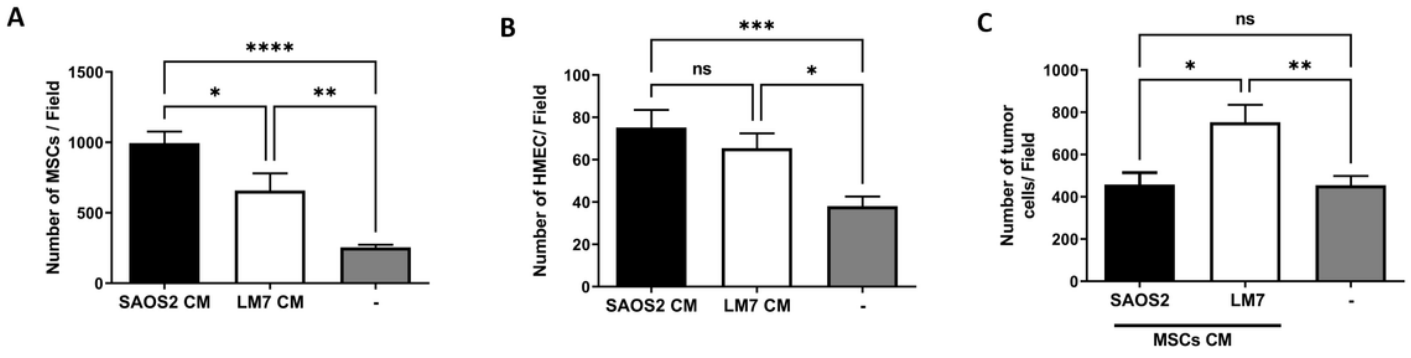

Figure 1

Chemotactic interplay between parenchymal and stromal cells in OS. **A.** Migratory response of MSCs towards the CM of SAOS2 and LM7 cells, revealed that MSCs migrated significantly more towards SAOS2 CM. **B.** Migratory response of HMEC-1 cells towards the CM of SAOS2 and LM7 cells, no significant differences were observed. **C.** Migratory behavior of SAOS2 and LM7 cells, towards MSCs´

secretome, and as seen LM7 cells migrated more towards MSCs CM. DMEM was used as negative control in all migration assays (-). One-way ANOVA, ns: no significant; *p<0.05, **p < 0.01, ***p<0.001, ****p<0.0001. Data are representative of 3 independent experiments.

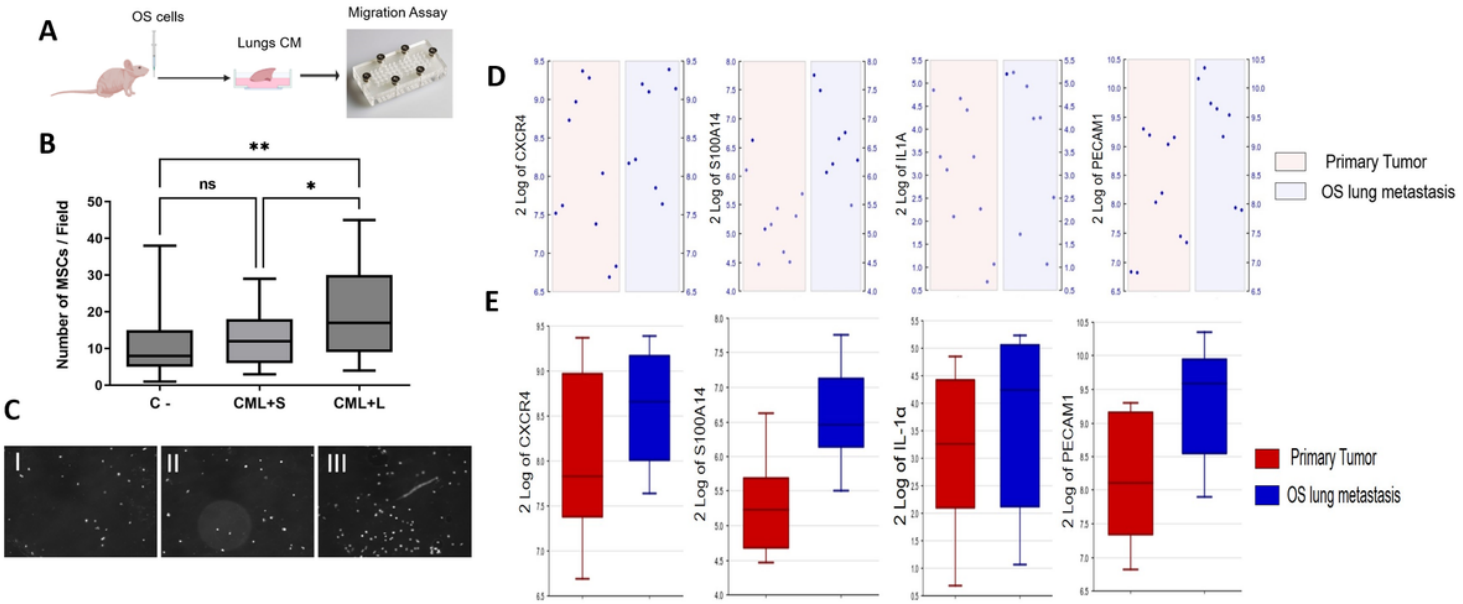

Figure 2

Migratory response of MSCs to CM from lungs of animals previously injected with SAOS2 or LM7 cells. **A.** Schematic illustration of the experimental design of the pulmonary OS metastasis and control groups in nude mice in order to obtain lungs CM. **B.** Migration of MSCs towards CM from lungs previously injected with OS cells. CML+S CM from lungs of animals previously injected with SAOS2; CML+L: CM from lungs of animals previously injected with LM7; C-: negative control. **C.** Representative images of DAPI stained MSCs migrating in response towards different conditions in B; **I** Negative control (-); **II**CML+S; **III** CML+L. **D.** Dot plots of CXCR4, S100A14, IL-1α, and PECAM1 from patients with metastatic OS and non-metastatic patients (GSE14359 dataset). **E.** Box plots of CXCR4, S100A14, IL-1α, and PECAM1 from patients with metastatic OS and non-metastatic patients show significantly higher expression in S100A14 and PECAM1 in metastatic samples, while CXCR4 and IL-1α displayed a similar trend (GSE14359 dataset). One-way ANOVA, ns: no significant; *p < 0.05, **p < 0.01. Data are representative of 3 independent experiments.

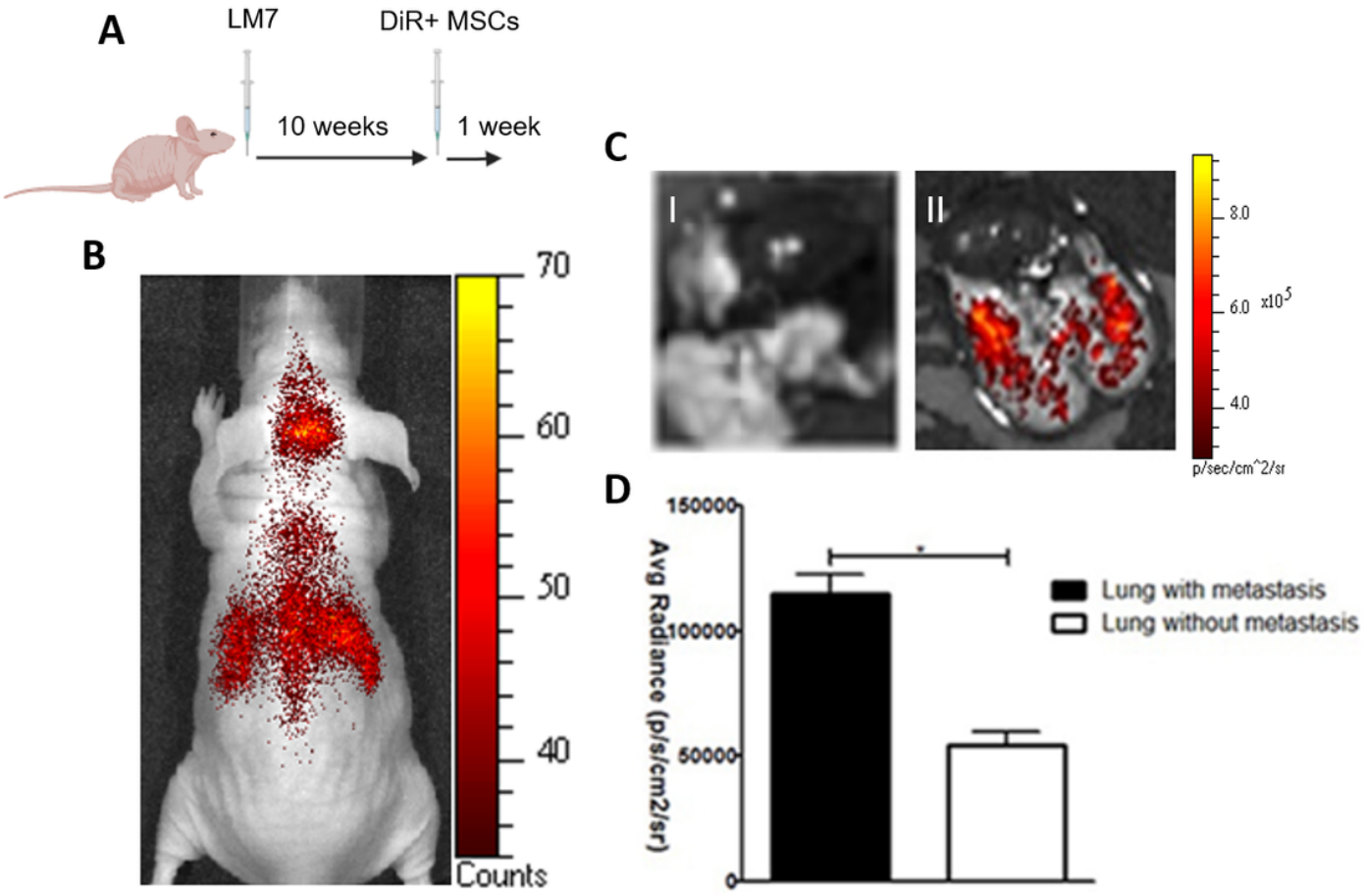

Figure 3

In vivo biodistribution of MSCs systemically administered 10 weeks after intravenous administration of tumor cells (LM7 cells), analyzed by FI. **A.**Schematic illustration of the experimental design of the in vivo experimental OS metastasis and MSCs homing ability in pulmonary environment. **B.**Whole-body biodistribution images of DiR pre-labeled MSCs, FI signal associated with presence of MSCs in lungs and brain. **C.** Representative images of lungs and heart of MSCs distribution in control or treated animals; **I**Lungs and heart of a control animal; **II** Lungs and heart of a micrometastatic bearing animal. The DiR signal detection and quantification (p / sec / cm2 / sr). **D.** DiR signal detection and quantification (p / sec / cm2 / sr) revealed a preferential homing into lungs previously colonized with metastatic cells (*p <0.05). t test, average ± SD.

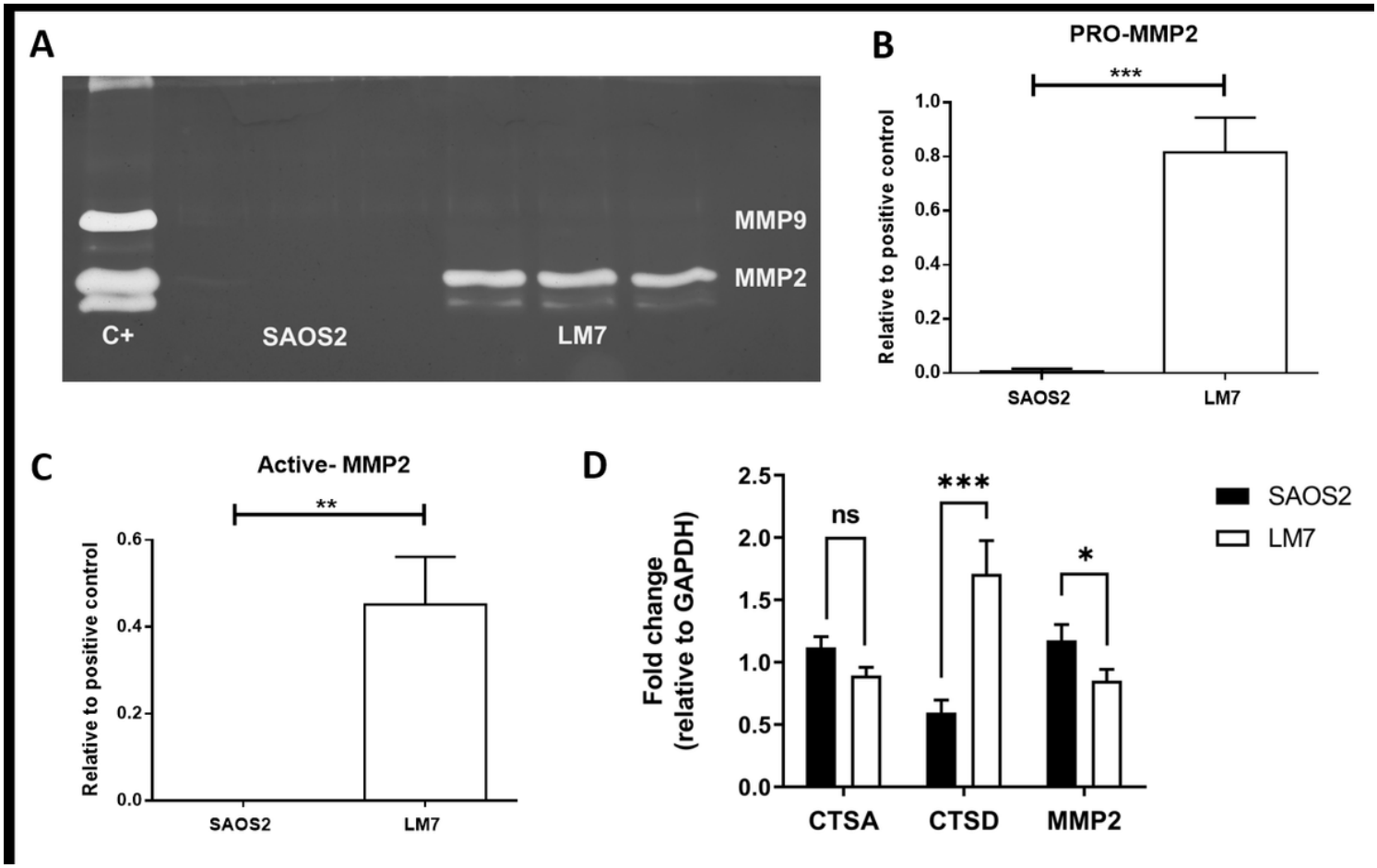

Figure 4

Characterization of the invasion-related phenotype of OS cells. **A.** Metalloproteinase activity in CM from SAOS2 and LM7 cells evaluated by zymography assay, CM from HT1080 cells was used as positive control (C+). MMP2 was detected and MMP9 was not detected in the CM from the parental or the metastatic cell line. **B.**Pro-MMP2 was significantly higher in the metastatic cell line LM7 than in SAOS2 cells. **C.** Active-MMP2 was only present in LM7 CM. **D.** qPCR analysis of cathepsin A (CTSA), cathepsin D (CTSD) and MMP2 revealed that LM7 cells had significantly higher CTSD mRNA levels than SAOS2 cells, while CTSA was similar in both cell lines. Regarding MMP2 expression, SAOS2 had higher expression of MMP2 at mRNA level. *T*-test, ns: no significant, * $p<0.05$, ** $p<0.01$, *** $p<0.001$. Data are representative of 3 independent experiments.

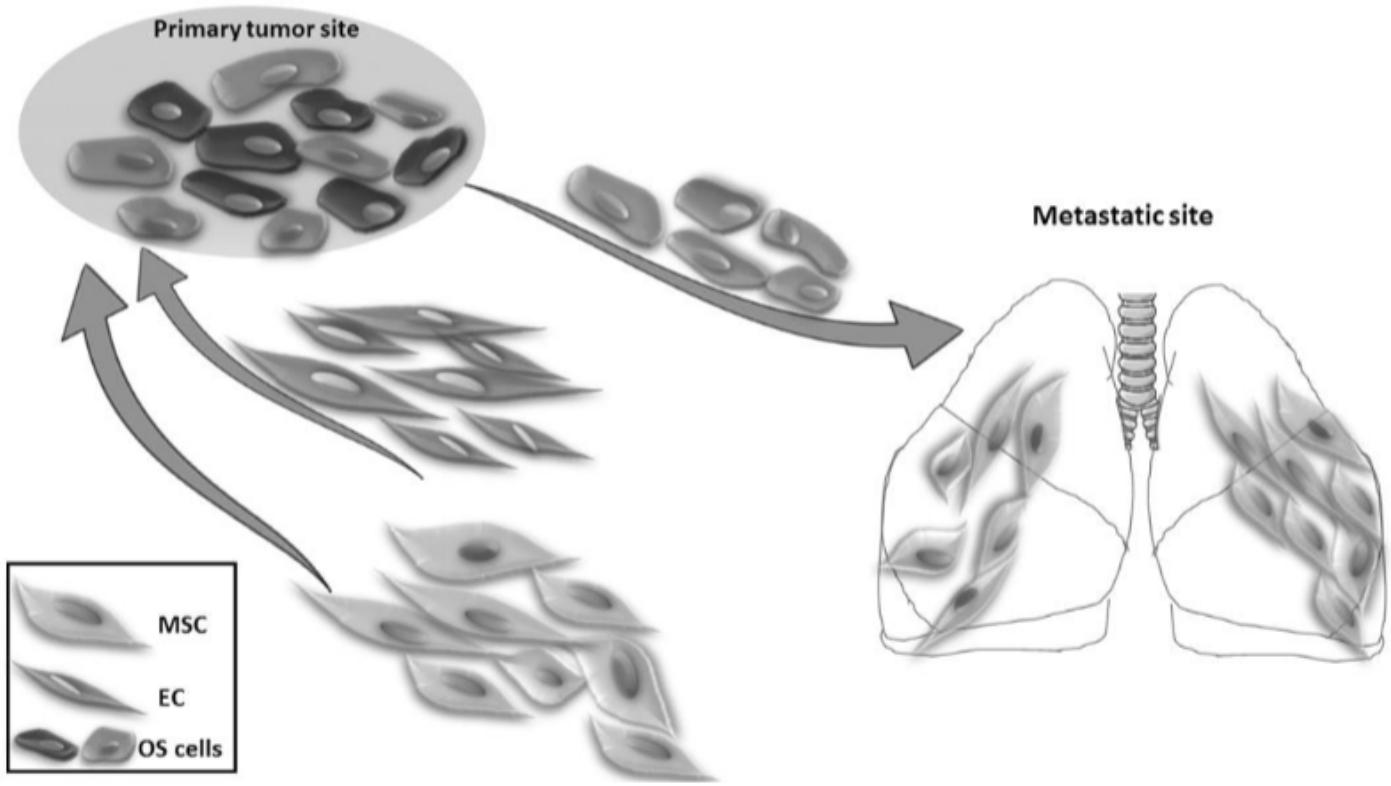

Figure 5

Proposed model on the interaction of MSCs and endothelial cells with OS cells within the primary site or secondary tumor growth. OS cells that reside at the primary tumor site recruit stromal cells, including MSCs and endothelial cells. OS cells with the ability to leave the primary tumor site and colonize new niches show improved migration towards MSCs, which would previously colonize the new niche (lung). MSCs (mesenchymal stem cells), EC (endothelial cells) and OS cells (osteosarcoma cells).

Supplementary Files

This is a list of supplementary files associated with this preprint. Click to download.

- SupplementaryFigure1.tif